Significant redox insensitivity of the functions of the SARS-CoV spike glycoprotein: comparison with HIV envelope.

Dimitri Lavillette, Rym Barbouche, Yongxiu Yao, Bertrand Boson, Cosset François-Loïc, Ian M Jones, Emmanuel Fenouillet

THE JOURNAL OF BIOLOGICAL CHEMISTRY VOL. 281, NO. 14, pp. 9200–9204, April 7, 2006

Significant Redox Insensitivity of the Functions of the SARS-CoV Spike Glycoprotein

*COMPARISON WITH HIV ENVELOPE**

Received for publication, November 22, 2005, and in revised form, January 11, 2006 Published, JBC Papers in Press, January 17, 2006, DOI 10.1074/jbc.M512529200

Dimitri Lavillette[‡1], Rym Barbouche[§¶1], Yongxiu Yao[‖], Bertrand Boson[‡], François-Loïc Cosset[‡], Ian M. Jones[‖], and Emmanuel Fenouillet[§2]

From [‡]INSERM U758, Ecole Normale Supérieure, Institut Fédératif de Recherche (IFR) 128, Lyon-Gerland F69007, Lyon, France, [§]IFR Jean-Roche, Faculté de Médecine Nord, F13015, Marseille, France, [¶]Institut Supérieur de Biotechnologie de Monastir, 5000 Monastir, Tunisia and [‖]School of Animal and Microbial Sciences, University of Reading, RG6 6AJ Reading, England, United Kingdom

The capacity of the surface glycoproteins of enveloped viruses to mediate virus/cell binding and membrane fusion requires a proper thiol/disulfide balance. Chemical manipulation of their redox state using reducing agents or free sulfhydryl reagents affects virus/cell interaction. Conversely, natural thiol/disulfide rearrangements often occur during the cell interaction to trigger fusogenicity, hence the virus entry. We examined the relationship between the redox state of the 20 cysteine residues of the SARS-CoV (severe acute respiratory syndrome coronavirus) Spike glycoprotein S1 subdomain and its functional properties. Mature S1 exhibited ~4 unpaired cysteines, and chemically reduced S1 displaying up to ~6 additional unpaired cysteines still bound ACE2 and enabled fusion. In addition, virus/cell membrane fusion occurred in the presence of sulfhydryl-blocking reagents and oxidoreductase inhibitors. Thus, in contrast to various viruses including HIV (human immunodeficiency virus) examined in parallel, the functions of the SARS-CoV Spike glycoprotein exhibit a significant and surprising independence of redox state, which may contribute to the wide host range of the virus. These data suggest clues for molecularly engineering vaccine immunogens.

SARS[3]-CoV is a new human coronavirus that causes a severe acute respiratory syndrome, sometimes with a fatal outcome. Its Spike glycoprotein is the major surface antigen and induces potent neutralizing antibodies (1–8). It is made up of S1 and S2 subdomains (2, 3). The S1 region interacts with angiotensin-converting enzyme 2 (ACE2), the primary cellular receptor (9–12), L-SIGN (13), and L-SECtin (14), whereas S2 mediates membrane fusion (2, 3). Here, we investigated the functional role of the 20 conserved cysteine residues of mature S1.

A variety of evidence has shown that the capacity of the viral envelope glycoproteins to mediate virus/cell membrane fusion depends on a precise thiol/disulfide balance within the viral surface complex (15–29). On one hand, manipulation of the native disulfide network of mature envelopes at the virus surface using reducing or alkylating reagents has important consequences for their subsequent capacity to carry out the virus/cell interaction process (15, 16, 19, 20, 23, 24, 26, and 28). On the other hand, natural and specific thiol/disulfide rearrangements occur within several viral envelopes to trigger conformational changes that insert the fusion peptide into the cell surface leading to virus entry (20, 21, 23, 25–27).

For HIV, gentle chemical reduction of Env efficiently prevents viral infectivity by inhibiting the capacity of the surface subunit (SU) to bind its ligands on the target cell surface (15, 19). In contrast, after receptor binding, fusion mediated by the transmembrane subunit occurs solely following reduction of SU by a cell-surface protein-disulfide isomerase (PDI) activity (19, 25–27). For these reasons, reducing or free sulfhydryl reagents and nonpermeant inhibitors of PDI (*e.g.* the thiol reagent DTNB and bacitracin, an oxidoreductive inhibitor) block entry (15, 19).

A proper disulfide network within MLV- and human T-leukemia virus-Env is also a determinant of virus entry. Incubation in the presence of dithiothreitol (DTT) of cell-bound virus inhibits Env fusogenicity. Sulfhydryl-blocking reagents also prevent virus/cell fusion, but entry can be rescued following disruption of a SU-transmembrane protein disulfide bond by appropriate chemical reduction *in vitro* (17, 20, 28). This has led to the proposal that triggering fusion requires for the protein disulfide bond between transmembrane protein and a *CXXC* thiol-reactive motif on SU to be isomerized within the *CXXC* sequence by the endogenous oxidoreductase activity supported by the motif.

In addition to these well documented retroviral examples, the E1 protein of the togavirus rubella (29) and the envelope of bovine viral diarrhea virus, a pestivirus, exhibit reactive thiols. The latter appears destabilized during the endocytosis to become fusogenic at an endosomal acidic pH following disulfide reduction via an unknown mechanism (21). For the Sindbis virus envelope glycoproteins, intact disulfide bonds are important for the stability and function of the envelope. The addition of DTNB alters fusion, whereas treatment using reducing reagents indicates that the cleavage of critical disulfides probably plays a role during the entry (23, 24). It is also important to note for the present study that redox changes probably control conformational rearrangements of some coronavirus proteins during cell interaction (22). Indeed, DTNB blocks mouse hepatitis virus entry by reaction with a free sulfhydryl in its S2 subunit, whereas chemical reduction enhances structural transitions associated with initiation of the fusion process (16, 22). Together, these results indicate that manipulation of the redox status of viral cysteine-rich envelope glycoproteins by either reducing or free

* This work was supported in part by a grant from the Agence Nationale de Recherche sur le SIDA (ANRS) (to E. F., I. M. J., and F.-L. C.), a fellowship from the ANRS (to R. B.), European Community Contract LSHB-CT-2004-005242, a grant from CONSERT (concerted safety and efficiency of retroviral transgenesis for gene therapy of inherited disease) (to F.-L. C.), and a grant from the Biotechnology and Biological Sciences Research Council (to I. M. J.). The costs of publication of this article were defrayed in part by the payment of page charges. This article must therefore be hereby marked "*advertisement*" in accordance with 18 U.S.C. Section 1734 solely to indicate this fact.

[1] These authors contributed equally to this work.

[2] Supported by ANRS Grant HCV 2006. To whom correspondence should be addressed: Faculté de Médecine Nord, Blvd. P. Dramard, F13015 Marseille, France. Tel./Fax: 33-491-69-88-47; E-mail: fenouillet.e@jean-roche.univ-mrs.fr.

[3] The abbreviations used are: SARS, severe acute respiratory syndrome; CoV, coronavirus; ACE2, angiotensin-converting enzyme 2; DTNB, 5,5′-dithiobis(2-nitrobenzoic acid); DTT, dithiothreitol; Env, envelope; GFP, green fluorescent protein; HIV, human immunodeficiency virus; MLV, murine leukemia virus; MPB, 3-(*N*-maleimidylpropionyl)biocytin; PBS, phosphate-buffered saline; PDI, protein-disulfide isomerase; SH, free sulfhydryl; SU, surface subunit; Tg, thyroglobulin.

sulfhydryl reagents strongly influences cell entry by a variety of enveloped viruses.

EXPERIMENTAL PROCEDURES

Reagents—DTNB, bacitracin, β-mercaptoethanol, DTT, porcine thyroglobulin (Tg), and other biochemical reagents were obtained from Sigma. The impermeant thiol reagent 3-(*N*-maleimidylpropionyl)biocytin (MPB) was from Molecular Probes (Eugene, OR). S1[4] was expressed using a recombinant baculovirus system and purified by protein A affinity chromatography. C-clade gp120 derived from the HIV_{CN54} isolate (a patient isolate) was expressed using a recombinant baculovirus system and purified by lectin-affinity chromatography (30). A secreted form of an ACE2-green fluorescent protein (GFP) fusion protein was also expressed using recombinant baculoviruses prior to purification from the tissue culture supernatant.

SDS-PAGE Analysis of MPB-labeled Sample—MPB is a sulfhydryl reagent coupled to biotin; its covalent interaction with protein thiols can be detected using a streptavidin-coupled staining system. S1 was incubated with MPB (0.1 mM, 30 min, 25 °C) or mock-treated. Quenching was performed using glutathione (0.2 mM, 10 min, 25 °C) and iodoacetamide (0.4 mM, 10 min, 25 °C). The sample was then analyzed by SDS-PAGE (8%). After blotting onto a nitrocellulose filter (Schleicher & Schuell) and blocking with phosphate-buffered saline (PBS), pH 7.4, 2% casein, 0.5% Tween 20, the filter was processed using streptavidin-coupled peroxidase (1:500, 30 min, 25 °C) and diaminobenzidine, as described previously (26, 30). Alternatively, staining of the filter was performed using Amido Black to assess the presence of contaminant proteins in the sample.

Thiol Content Determination—Samples containing Tg, S1, or gp120 diluted in PBS (250 ng/10 μl of PBS) were dot-blotted onto a nitrocellulose filter. After blocking with PBS, 0.5% casein, 0.5% Tween 20 and washing, filters were incubated with MPB (0.1 mM, 30 min, 25 °C). Similar results were obtained when the antigens were incubated with MPB prior to dot-blotting. After washing, the filter was incubated with streptavidin-coupled peroxidase (Amersham Biosciences, 1:500) for 30 min and then after washing again, labeling was performed using diaminobenzidine (Sigma). Spot intensity was then quantified by densitometry using a PhosphorImager and its accompanying software (Amersham Biosciences). The relationship between the measured spot intensity and the thiol content of the sample of interest was assessed using a reference curve obtained as follows. Increasing amounts of Tg, previously submitted to reduction following β-mercaptoethanol treatment, were dot-blotted and subsequently MPB-labeled as described above. Tg was used as this glycoprotein exhibits a similar "cysteine to molecular weight" ratio to S1 and gp120. Densitometry of the resulting Tg spots produced a linear dose-response curve between 1 and 50 ng. Taking into account its molecular mass (about 300 kDa) and cysteine content (122 cysteine residues/molecule), we obtained a standard curve that enabled the assignment of a specific thiol content to the measured densitometry value of the sample within the range of 0.3 to 10 pmol (26, 30). The signal/background ratio was typically about 50.

Controlled Chemical Reduction—The sample was treated with increasing concentrations of β-mercaptoethanol (10 min at 25 °C) before dot-blotting, MPB labeling, and further processing to assess its thiol content as described above. For binding experiments, the sample was treated with β-mercaptoethanol (10 min at 25 °C) prior to incubation with iodoacetamide (≥3:1 iodoacetamide/β-mercaptoethanol ratio; 30 min at 25 °C). β-mercaptoethanol, which interferes with receptor interaction, was removed under vacuum. The sample was then processed for receptor binding as described below and elsewhere (26, 30). Treatment with DTT was similarly performed.

Receptor Binding Assays—For ACE2 binding, microtitration plates were coated with soluble ACE2 (500 ng/100 μl of 200 mM sodium bicarbonate, pH 8.2) for 24 h at 21 °C. The plate was washed three times with 10 mM Tris-HCl, pH 7.4, 150 mM NaCl, 5% w/v casein (TBC). Purified S1 was diluted in TBC and incubated with ACE2 in the plate for 1 h. After washes, anti-human Ig conjugated to horseradish peroxidase (1:1000 in TBC) was added for 1 h, and the plate was finally incubated with 3,3′,5,5′-tetramethylbenzidine chromogenic substrate (Europa Bioproducts).

For CD4 binding (described in detail in Ref. 26), soluble HIV SU (100 ng/100 μl) was incubated for 2 h in microtitration plates coated with D7324 (an anti-C terminus antibody) (Aalto, Dublin, Ireland); ^{125}I-CD4 (2×10^4 cpm/well) was then added for 2 h. After washes, radioactivity was counted. Background binding was measured as the signal generated by similar wells lacking Env.

Pseudotyped Virus Infection—The various pseudotyped particles used in this study were generated and produced according to a general protocol described previously (31). Briefly, 293T cells were transfected using a calcium phosphate transfection kit (Clontech) with expression vectors encoding the various viral envelope glycoproteins, core/packaging components, and a retroviral transfer vector harboring the gene encoding GFP. Supernatants that contained pseudotyped particles were harvested 36 h post-transfection and used for envelope expression following filtration. An MLV core was used for SARS-CoV-, MLV-, and HIV712-(a truncated HIV_{NL4-3} envelope with no cytoplasmic tail) envelope expression.

Cells (8×10^4) were seeded in a 12-well plate and infected 24 h later with 100 μl of virus supernatant in a final volume of 400 μl. VeroE6 cells were used for SARS-CoV- and MLV-pseudotyped infections. HeLaP4 (CD4 positive) cells were used for HIV-pseudotyped infection. The drugs or reagents from a 10× stock solution were added during the infection step. Alternatively, the drugs were preincubated with the virus sample or cells for 1–3 h prior to cell/virus coincubation. After 5 h of coincubation, the supernatants were removed and the cells incubated in culture medium for 72 h at 37 °C. GFP expression was determined by fluorescence-activated cell sorter analysis. The infectivity of pseudotyped particles incubated with drugs or neutralizing antibodies was compared with the infectivity observed using a medium containing Dulbecco's modified Eagle's medium-10% fetal calf serum only and standardized to 100%.

RESULTS

Free Sulfhydryls Are Present on Mature S1—We first investigated the involvement in disulfide bond formation of the 20 cysteine residues present on a mature, recombinant form of S1. We produced and purified a recombinant glycoprotein (similar to that described in Ref. 10) for biochemical studies because the soluble S1 antigen could not be isolated from a virus preparation. This form of recombinant protein was used for the original description of ACE2 as the virus receptor (10) and in a number of subsequent studies examining binding activity, folding, and even the role of the disulfides of S1 (32, 33). The purity of the sample and the presence of free thiols were examined using SDS-PAGE analysis and Western blotting. A single molecular species migrating as the S1 recombinant antigen was found to react with MPB. This thiol reagent is coupled to biotin, and its reaction with the protein thiols was detected using streptavidin-coupled peroxidase and diaminobenzidine (Fig. 1*A*).

[4] S1-Fc is similar to an antigen that was first described by Li *et al.* (10).

We then measured the quantity of free thiols detected on S1 following MPB labeling, SDS-PAGE, and Western blotting. Purified S1 was dot-blotted and labeled using MPB as described above. Spot intensity was measured by densitometry, and the free sulfhydryl content corresponding to the signal was quantified using a standard curve obtained as described above and elsewhere (26, 30). We found that an average of 4 SH were present per S1 antigen. This result was consistent with the fact that about 4 of 20 cysteine residues of mature S1 were present as unpaired cysteines in contrast to HIV Env, examined in parallel, where all cysteine residues were disulfide-bonded (Fig. 1*B*). The data obtained for HIV SU, which exhibits a similar number of cysteine residues in its amino acid sequence, are in agreement with those reported previously (26).

Low Sensitivity of S1 to Chemical Reduction—We next examined the susceptibility of S1 to increasing concentrations of β-mercaptoethanol and determined the thiol content following the chemical reduction as before. HIV Env was examined in parallel. S1 exhibited a higher sensitivity to the reducing agent than HIV Env (Fig. 2*A*). From these studies, a relationship between the concentration of β-mercaptoethanol and the thiol content of the protein induced by the presence of the reducing agent was established, and we prepared samples exhibiting a defined amount of reduced bonds per molecule. After treatment with the β-mercaptoethanol concentrations determined previously, aliquots (250 ng) from each condition were processed to confirm the expected thiol content of each sample using dot-blot, MPB labeling, staining, and thiol quantitation as described above and in Ref. 30. The rest of the sample (~5 μg) was incubated with iodoacetamide and the reducing agent removed under vacuum. The resulting antigen was assayed for receptor binding.

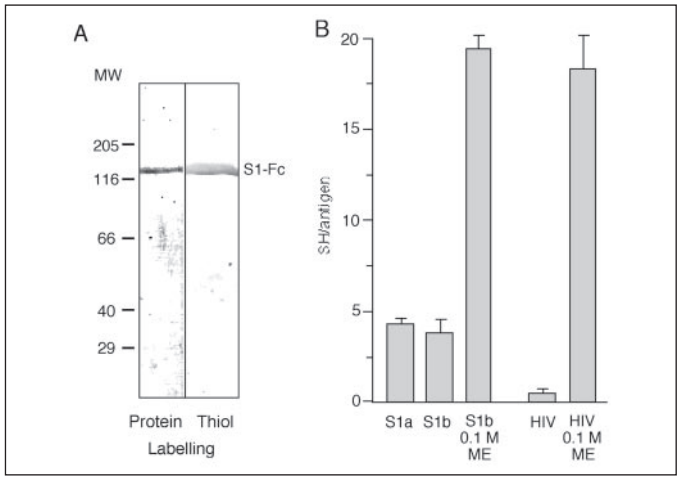

FIGURE 1. **Thiol content of mature S1.** *A,* purity**.** The S1 recombinant antigen was incubated with MPB prior to 8% SDS-PAGE and Western blotting. The filter was incubated with Amido Black (*Protein labeling*) or streptavidin-peroxidase/diaminobenzidine (*Thiol labeling*). *B,* thiol content. S1 (two batches, S1a and S1b) and HIV_{CN54} Env were dot-blotted and labeled with MPB. The thiol content per molecule was quantified by densitometry using a standard curve; β-mercaptoethanol (*ME*) treatment produced fully reduced antigens ($n = 4$; means are shown).

Chemically reduced, iodoacetamide-treated S1 displaying about half of its cysteine residues as unpaired residues (*i.e.* a total of about 10 SH per antigen) continued to bind ACE2 (Fig. 2*B*) in contrast to reduced HIV Env, which lost CD4 receptor binding when more than one disulfide per SU was reduced, confirming the data reported previously (26). Higher levels of unpaired cysteine residues on S1 altered the ACE2 binding capacity, although a specific interaction was still detected when S1 exhibited 75% of its cysteine residues as unpaired residues. Complete reduction showed essentially no binding capacity together with poor reaction with human polyclonal antibodies (data not shown), suggesting general denaturation.

The S1-dependent Membrane Fusion Process Is Significantly Redox-insensitive—We confirmed, using a biologically relevant system and a native virus surface-associated form of the Spike antigen, the low susceptibility of ACE2 binding toward reduction as observed in Fig. 2*B*. In addition, we examined the effect of chemical reduction on the fusion capacity of the Spike complex.

We developed an infection assay to address the Spike-mediated entry into $ACE2^+$ VeroE6 cells of MLV viruses pseudotyped with Spike and carrying the GFP gene (see above). In this system, GFP expression by target cells is induced following the virus entry and quantified by flow cytometry. This assay is able to measure the antiviral activity of inhibitors targeting the Spike-mediated steps, *e.g.* home-made specific rabbit-neutralizing antisera raised against S1-Fc (Fig. 3). For chemical reduction, we used DTT because this reagent is widely used for this procedure in cell culture. Preliminary experiments defined concentrations that were noncytotoxic (data not shown).

First, we examined the effect of 0.6 mM DTT on virus entry. Pretreatment of the virus, pretreatment of the cells, or addition of the reducing agent during the coincubation step of pseudotyped particles and VeroE6 cells did not significantly modify the subsequent expression of GFP (Fig. 3). Thus, although 0.6 mM DTT produced an S1 antigen exhibiting half of its cysteine residues as unpaired residues (the thiol content of the antigen following the treatment was assessed as described above), the overall capacity of the Spike complex to mediate fusion was

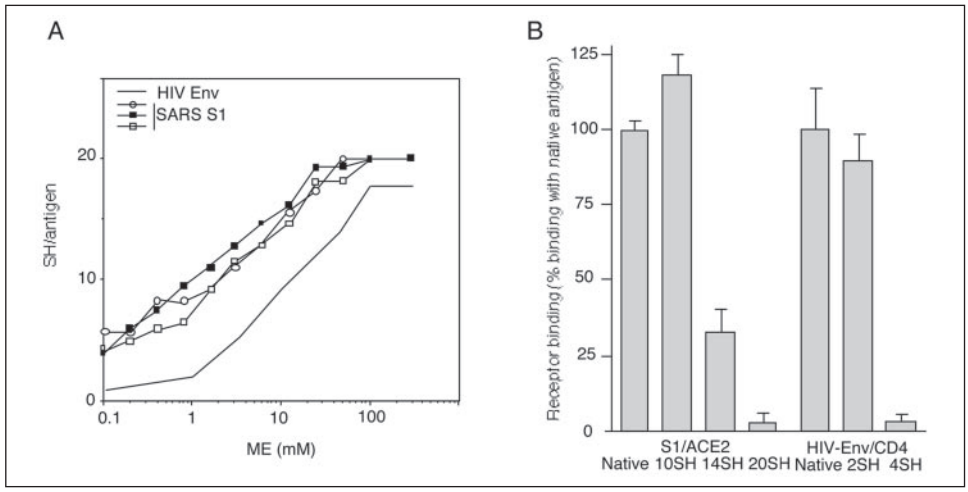

FIGURE 2. **Thiol content and ACE2 binding.** *A,* chemical reduction. S1 and HIV SU were treated using increasing concentrations of β-mercaptoethanol (*ME*). The thiol content was determined as described for Fig. 1*B* (S1, $n = 3$; HIV SU, mean of $n = 2$). *B,* receptor binding. S1 was either mock-treated (*Native*; ~4 SH/antigen) or chemically reduced as described in *A* to induce ~6 - 16 additional SH/antigen. ACE2 binding was assessed using an enzyme-linked immunosorbent assay based on soluble ACE2 for coating. HIV SU was either mock-treated (native; 0 SH) or chemically reduced (~2–4 SH/antigen); ^{125}I-recombinant soluble CD4 binding was assessed. Processing of the samples enabled to reach nonactive concentrations of reducing agent during the binding reaction (26, 30).

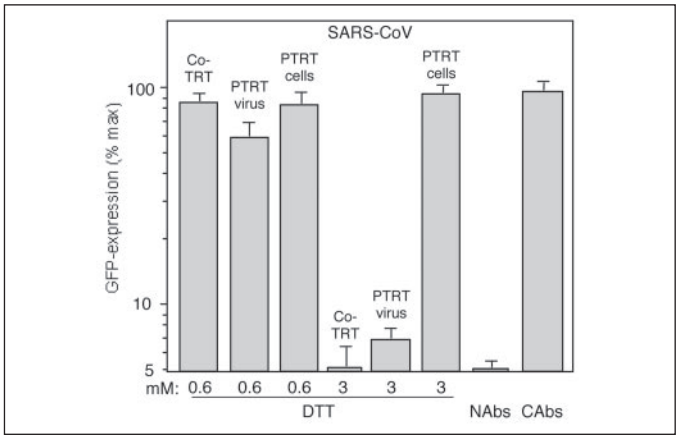

FIGURE 3. **Thiol content and Spike-mediated fusion.** DTT treatment at indicated concentrations was performed during infection of VeroE6 cells with SARS-CoV pseudovirus (*CoTRT*). Alternatively, virions (*PTRT virus*) or cells (*PTRT cells*) were pretreated using DTT prior to dilution and subsequent infection. For infection, cells and virions carrying the GFP gene were coincubated for 4 h before washing and culture for 72 h. Cell expression of GFP resulting from virus entry was quantified using flow cytometry. The capacity of the assay to detect inhibition of virus entry was measured using anti-SARS neutralizing antisera. The infectivity in each condition was compared with the infectivity of untreated pseudotypes standardized to 100% (n = 3–5; duplicates were performed; one experiment is shown). *NAbs*, neutralizing antibodies; *CAbs*, control antibodies.

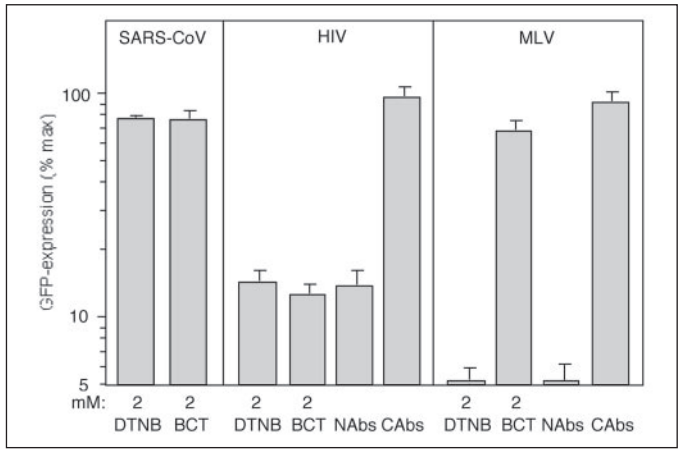

FIGURE 4. **Redox shuffling and fusion.** Infections were performed essentially as described for Fig. 3. VeroE6 cells were used for SARS-CoV and MLV pseudotype infection. HeLaP4 CD4+ cells were used for HIV_{NL4-3} pseudotype infection. Efficient, noncytotoxic, concentrations of DTNB and bacitracin (*BCT*) were added during the coincubation step of cells and vectors (15, 19). *NAbs*, neutralizing antibodies; *CAbs*, control antibodies.

preserved. Lower concentrations of DTT (≤0.3 mM) did not modify GFP expression, indicating that the reduction of the few S1 disulfides obtained in these conditions did not improve or inhibit pseudotyped virus entry (data not shown). Notably, this result showed that these treatments did not improve the fusion competence of Spike in contrast to other viral envelopes for which fusion capacity is triggered by gentle chemical reduction (*cf.* Introduction).

Second, we studied the effect of 3 mM DTT, which gave rise to an S1 antigen exhibiting 75% of its cysteine residues as unpaired residues. Pretreatment of the virus or addition of the reducing agent during the coincubation step of virus and cells prevented virus entry. Pretreatment of cells with 3 mM DTT followed by dilution prior to infection did not modify GFP expression, hence virus entry, indicating that such a concentration did not affect infection via interference with a cell-surface component.

These data are consistent with two observations: (i) S1 exhibiting half of its cysteine residues as unpaired residues binds ACE2 (Fig. 2*B*); (ii) site-directed mutagenesis of either Cys-323 or Cys-378 has no effect on the binding of S1 to ACE2 (32) leading to the conclusion that both the binding and fusion capacity of the Spike complex are significantly reduction insensitive. These results indicate that the unpaired cysteine residues of S1 (Fig. 1*B*) and ACE2 binding dispensable disulfides (Figs. 2*B* and 3) have no role in the biological activity of mature S1 (32). Alternatively, they are consistent with the possibility that unpaired cysteines and binding dispensable disulfides act as donor/acceptor as part of redox reactions, which may occur within the Spike complex or between the complex and cell-surface proteins to activate fusogenicity, hence contributing to entry.

We examined this possibility using DTNB, a compound that reacts with free sulfhydryls and bacitracin, a PDI inhibitor (Fig. 4). Neither compound affected the infection, indicating that unpaired cysteines and redox shuffling within Spike and/or cell proteins have no role during entry. We ensured that our pseudotyping assay enabled the study of redox-sensitive fusion: (i) DTNB and bacitracin inhibit infection by vectors pseudotyped with HIV Env, in agreement with the role of reactive thiols (blocked by DTNB) associated with cell-surface PDI (blocked by bacitracin) in HIV entry via the SU reduction by PDI (15, 19); (ii) DTNB, not bacitracin, inhibits MLV Env-mediated fusion, which is consistent with an autocatalytic disulfide shuffling (blocked by DTNB) within Env that triggers entry (20).

DISCUSSION

The Spike glycoprotein of SARS-CoV is a major target for neutralizing antibodies, and the development of a vaccine preparation would probably include molecularly engineered forms of recombinant SARS-CoV Spike immunogens (1–8). In the event of another outbreak, it is therefore important to obtain information on the biochemical characteristics of the Spike that govern its biologically active conformation.

The SARS-CoV envelope is organized into the S1 outer region that encompasses the receptor-binding domain and the S2 transmembrane region, which mediates membrane fusion (2, 3). Various viral envelopes, including those of retroviruses and coronaviruses, exhibit a comparable functional architecture. Despite these common features and in contrast to the envelope-mediated entry of several viruses (*cf.* Introduction), our work indicates that the involvement of the complete complement of cysteine residues of mature Spike in disulfides and redox changes within SARS-CoV Spike and cell-surface molecules are not obligatory for virus entry. However, the observation that ~3 disulfides of mature S1 are dispensable for ACE2 binding does not rule out the possibility that the corresponding bridges play a role during the intracellular biosynthetic pathway, especially folding, and such a potential role may explain Cys residue conservation.

The independence of ACE2 binding toward disulfide bonding (this study) and the finding that mutagenesis of several amino acid residues only marginally affects receptor binding (32, 34) are consistent with two recent observations: the key residues involved in the contacts between the concave S1 and the convex ACE-2 surfaces are few, and only two cysteine residues (Cys-467 and Cys-474) are present within the receptor binding motif, which makes all the contact with ACE2 (9). These characteristics, the fact that the S1 protein is a relatively large molecule (2) and the innate instability of its disulfide bonds (Fig. 2*A*), may be properties that allow the envelope complex to be flexible and escape dependence on redox reactions induced by cell-surface catalysts prior to entry. Such independence toward the redox changes may be part of the reason for the wide host range of the virus and contributed to the zoonosis that led to human infection (35, 36).

The lack of effect of blocking the free sulfhydryls of the SARS-CoV

envelope protein using DTNB raises the question of the functions of the unpaired cysteine residues. Although the cysteine residues present in the Spike complex are quite conserved between civet and human isolates (9), the lack of an effect by DTNB indicates that they are unlikely to have a functional role as part of a virus/cell interaction process, at least not as a donor or acceptor during redox shuffling reactions.

In addition to contributing to a fuller understanding of SARS virus entry and, by extension, that of other coronaviruses, our study should aid the design of recombinant vaccine immunogen based on the Spike protein. In particular, together with recent crystal structural data (9), our results suggest that the engineering of cysteine residues to improve immune presentation or stability may not adversely affect the biological conformation of the protein.

The location of the unpaired cysteine residues discovered in this study is not known, but it is possible that, in so large a molecule, their oxidation is prevented by the surrounding protein fold. Conceivably, unpaired cysteine residues are available for the creation of additional bonding at some stage of envelope evolution, and such plasticity may have contributed to the capacity of this coronavirus to infect many species (35, 36) and adapt to human cell-surface ligands (9, 33).

Acknowledgments—We are grateful to Valerie Bosch for providing HIV-Env-expressing plasmid and to Willy Spaan and Jeroen Corver for developing SARS-CoV Spike-expressing plasmid.

REFERENCES

1. Temperton, N. J., Chan, P. K., Simmons, G., Zambon, M. C., Tedder, R. S., Takeuchi, Y., and Weiss, R. A. (2005) *Emerg. Infect. Dis.* **11,** 411–416
2. Xiao, X., and Dimitrov, D. S. (2004) *CMLS Cell. Mol. Life Sci.* **61,** 2428–2430
3. Petit, C. M., Melancon, J. M., Chouljenko, V. N., Colgrove, R., Farzan, M., Knipe, D. M., and Kousoulas, K. G. (2005) *Virology* **341,** 215–230
4. Bisht, H., Roberts, A., Vogel, L., Subbarao, K., and Moss, B. (2005) *Virology* **334,** 160–165
5. Faber, M., Lamirande, E. W., Roberts, A., Rice, A. B., Koprowski, H., Dietzschold, B., and Schnell, M. J. (2005) *J. Gen. Virol.* **86,** 1435–1440
6. He, Y., Zhu, Q., Liu, S., Zhou, Y., Yang, B., Li, J., and Jiang, S. (2005) *Virology* **334,** 74–82
7. Yao, Y. X., Ren, J., Heinen, P., Zambon, M., and Jones, I. M. (2004) *J. Infect. Dis.* **190,** 91–98
8. Pang, H., Liu, Y., Han, X., Xu, Y., Jiang, F., Wu, D., Kong, X., Bartlam, M., and Rao, Z. (2004) *J. Gen. Virol.* **85,** 3109–3113
9. Li, F., Li, W., Farzan, M., and Harrison, S. C. (2005) *Science* **309,** 1864–1868
10. Li, W., Moore, M. J., Vasilieva, N., Sui, J., Wong, S. K., Berne, M. A., Somasundaran, M., Sullivan, J. L., Luzuriaga, K., Greenough, T. C., Choe, H., and Farzan, M. (2003) *Nature* **426,** 450–454
11. Fukushi, S., Mizutani, T., Saijo, M., Matsuyama, S., Miyajima, N., Taguchi, F., Itamura, S., Kurane, I., and Morikawa, S. (2005) *J. Gen. Virol.* **86,** 2269–2274
12. Ng, M. L., Tan, S. H., See, E. E., Ooi, E. E., and Ling, A. E. (2003) *J. Gen. Virol.* **84,** 3291–3303
13. Jeffers, S. A., Tusel, S. M., Gillim-Ross, L., Hemmila, E. M., Achenbach, J. E., Babcock, G. J., Thomas, W. D., Thackray, L. B., Young, M. D., Mason, R. J., Ambrosino, D. M., Wentworth, D. E., Demartin, J. C., and Holmes, K. V. (2004) *Proc. Natl. Acad. Sci. U. S. A.* **101,** 15748–15753
14. Gramberg, T., Hofmann, H., Moller, P., Lalor, P. F., Marzi, A., Geier, M., Krumbiegel, M., Winkler, T., Kirchhoff, F., Adams, D.H., Becker, S., Munch, J., and Pohlmann, S. (2005) *Virology* **340,** 224–236
15. Ryser, H. J., Levy, E. M., Mandel, R., and DiSciullo, G. J. (1994) *Proc. Natl. Acad. Sci. U. S. A.* **91,** 4559–4563
16. Gallagher, T. M. (1996) *J. Virol.* **70,** 4683–4689
17. Pinter, A., Kopelman, R., Li, Z., Kayman, S. C., and Sanders, D. A. (1997) *J. Virol.* **71,** 8073–8077
18. Sanders, D. A. (2000) *Subcell. Biochem.* **34,** 483–514
19. Fenouillet, E., Barbouche, R., Courageot, J. C., and Miquelis, R. (2001) *J. Infect. Dis.* **183,** 744–752
20. Wallin, M., Ekstrom, M., and Garoff, H. (2004) *EMBO J.* **23,** 54–65
21. Krey, T., Thiel, H. J., and Rümenapf, T. (2005) *J. Virol.* **79,** 4191–4200
22. Sturman, L. S., Ricard, C. S., and Holmes, K. V. (1990) *J. Virol.* **64,** 3042–3050
23. Abell, B. A., and Brown D. T. (1993) *J. Virol.* **67,** 5496–5501
24. Anthony, R. P., Paredes, A. M., and Brown, D. T. (1992) *Virology* **190,** 330–336
25. Gallina, A., Hanley, T. M., Mandel, R., Trahey, M., Broder, C. C., Viglianti, G. A., and Ryser, H. J. (2002) *J. Biol. Chem.* **277,** 50579–50588
26. Barbouche, R., Miquelis, R., Jones, I. M., and Fenouillet, E. (2003) *J. Biol. Chem.* **278,** 3131–3136
27. Markovic, I., Stantchev, T. S., Fields, K. H., Tiffany, L. J., Tomic, M., Weiss, C. D., Broder, C. C., Strebel, K., and Clouse, K. A. (2004) *Blood* **103,** 1586–1594
28. Wallin, M., Ekstrom, M., and Garoff, H. (2005) *J. Virol.* **79,** 1678–1685
29. Gros, C., Linder, M., and Wengler, G. (1997) *Virology* **230,** 179–186
30. Barbouche, R., Lortat-Jacob, H., Jones, I. M., and Fenouillet, E. (2005) *Mol. Pharmacol.* **67,** 1111–1118
31. Bartosch, B., Dubuisson, J., and Cosset, F. L. (2003) *J. Exp. Med.* **197,** 633–642
32. Wong, S. K., Li, W., Moore, M. J., Choe, H., and Farzan, M. (2004) *J. Biol. Chem.* **279,** 3197–3201
33. Li, W., Zhang, C., Sui, J., Kuhn, J.H., Moore, M. J., Luo, S., Wong, S. K., Huang, I. C., Xu, K., Vasilieva, N., Murakami, A., He, Y., Marasco, W. A., Guan, Y., Choe H., Farzan, M. (2005) *EMBO J.* **24,** 1634–1643
34. Chakraborti, S., Prabakaran, P., Xiao, X., and Dimitrov, D. S. (2005) *Virol. J.* **2,** 73–83
35. Poon, L. L., Chu, D. K., Chan, K. H., Wong, O. K., Ellis, T. M., Leung, Y. H., Lau, S. K., Woo, P. C., Suen, K. Y., Yuen, K. Y., Guan, Y., and Peiris, J. S. (2005) *J. Virol.* **79,** 2001–2009
36. Martina, B. E., Haagmans, B. L., Kuiken, T., Fouchier, R. A., Rimmelzwaan, G. F., Van Amerongen, G., Peiris, J. S., Lim, W., and Osterhaus, A. D. (2003) *Nature* **425,** 915

Significant Redox Insensitivity of the Functions of the SARS-CoV Spike Glycoprotein: COMPARISON WITH HIV ENVELOPE

Dimitri Lavillette, Rym Barbouche, Yongxiu Yao, Bertrand Boson, François-Loïc Cosset, Ian M. Jones and Emmanuel Fenouillet

J. Biol. Chem. 2006, 281:9200-9204.
doi: 10.1074/jbc.M512529200 originally published online January 17, 2006
